

subsequent dredge-up episode [8].

For AGB stars of 1-7 solar masses, models indicate that the main source of Na, at solar metallicity, is a ^{23}Na pocket, located right below the hydrogen burning shell [8]. At lower metallicities, other mechanisms, such as neutron capture on ^{22}Ne may become important [9].

Another scenario where the $^{22}\text{Ne}(p,\gamma)^{23}\text{Na}$ reaction is active are classical novae explosions. A recent study showed that the $^{22}\text{Ne}(p,\gamma)^{23}\text{Na}$ reaction rate uncertainty strongly affects the final abundances of neon, sodium and magnesium isotopes, demonstrating the need for new experimental efforts on the $^{22}\text{Ne}(p,\gamma)^{23}\text{Na}$ cross section [10].

2 LUNA: Laboratory for Underground Nuclear Astrophysics

The Laboratory for Underground Nuclear Astrophysics has been designed to measure nuclear reactions cross sections at energies inside the Gamow Peak; it is located deep underground in the Gran Sasso National Laboratory, where the signal to background ratio is not affected by cosmic ray interactions within detectors [11].

The Gran Sasso underground facility is shielded against cosmic rays by a rock cover (1400 m thick) equivalent to 3800 m of water, suppressing the muon and neutron flux by six and three orders of magnitude, respectively.

The measurement of the cross section and the determination of the astrophysical S - factor for thermonuclear reactions require an experimental apparatus composed of an accelerator, a target, and a detection system.

The LUNA 400 kV accelerator delivers a proton beam of $500\mu\text{A}$ or an alpha beam of $300\mu\text{A}$ in the energy range of $E_p = 50\text{-}400\text{ keV}$. The ions can be sent into one of two different beam lines, thereby allowing the parallel installation of solid and gas target setups.

3 Experimental setup

The experimental setup for the $^{22}\text{Ne}(p,\gamma)^{23}\text{Na}$ experiment, consists of a windowless gas target with three differential pumping stages and a gas purification and recirculation system [12].

3.1 Target density study

The reaction yield is directly proportional to the target density (see eq. 1).

$$Y = \int_{z_1}^{z_2} \rho(z)\sigma(E(z))\eta(z)dz \quad (1)$$

where z_1 and z_2 are the initial and final position of the target, $\sigma(E(z))$ is the cross section at the energy $E(z)$ and $\eta(z)$ is the absolute detection efficiency for a γ -ray of the given energy originating at position z .

In the case of an extended gas target it is of crucial importance to know the particle density in the area where

Table 1. Summary of the explored $^{22}\text{Ne}(p,\gamma)^{23}\text{Na}$ resonances

$E_{level}[\text{keV}]$	$E_{res}^{LAB}[\text{keV}]$	$\omega\gamma[\text{eV}]$ Görres [3]	$\omega\gamma[\text{eV}]$ Hale [5]	LUNA
8862	71	$\leq 4.2\cdot 10^{-9}$	$\leq 1.9\cdot 10^{-10}$	u.l.
8894	104	$\leq 6.0\cdot 10^{-7}$	$\leq 1.4\cdot 10^{-7}$	u.l.
8946	159	$\leq 6.5\cdot 10^{-7}$	$\leq 9.2\cdot 10^{-9}$	detected
8972	186	$\leq 2.6\cdot 10^{-6}$	$\leq 2.6\cdot 10^{-6}$	detected
9000	215	$\leq 1.4\cdot 10^{-6}$	$\leq 1.4\cdot 10^{-6}$	u.l.
9039	256	$\leq 2.6\cdot 10^{-6}$	$\leq 1.3\cdot 10^{-7}$	detected

the beam passes through the target.

To obtain a density profile along the beam path a first set of measurements of pressure and temperature without the beam and, in a second run, a density study with the proton beam, using the resonance scan technique and a NaI detector, have been performed. Two different setups have been used.

For the measurement without the beam a dedicated INOX target chamber and an interconnecting tube have been appositely realized with several flanges used to connect pressure and temperature gauges. The density profile without beam has been determined with an uncertainty of 1.1%.

The density of the target gas may decrease along the beam path due to heat transfer from the intense ion beam. In order to study the beam heating effect a similar setup was used with a target chamber and a NaI detector. The narrow resonance at $E_p = 271.6\text{ keV}$ in the $^{21}\text{Ne}(p,\gamma)^{22}\text{Na}$ reaction has been used. For a given gas pressure and beam current I, the proton beam energy has been changed in 1-3 keV steps in order to populate the resonance at different positions along the beam axis and to find the proton beam energy corresponding to the resonance in front of the detector. Finally the experimental gas target density can be calculated from the experimental energy loss and compared with the number density of the target gas without beam heating corrections. As a result, the beam heating effect in neon gas has been found to be smaller than in other gases (i.e. ^{14}N) [13].

3.2 Setup for the resonances study

The final setup for the $^{22}\text{Ne}(p,\gamma)^{23}\text{Na}$ HPGe phase consisted of two HPGe detectors, one at 90° with respect to the beam direction, and the other one at 55° effective angle. The use of two high resolution detectors with well defined solid angles allow a measurement not only of the total resonance strength, but also of the different branching ratios of the resonance decay. The two detectors are surrounded by a 4 cm thick copper shielding and a 25 cm thick lead shielding in order to suppress the environmental background.

The gamma detection efficiency has been determined in the energy range of interest for the measurement (i.e. $440\text{ keV} < E_\gamma < 9.5\text{ MeV}$) with the radioactive sources at the lower energies (^7Be , ^{137}Cs , ^{60}Co and ^{88}Y) and with the $^{14}\text{N}(p,\gamma)^{15}\text{O}$ [14] nuclear reaction at the higher energies.

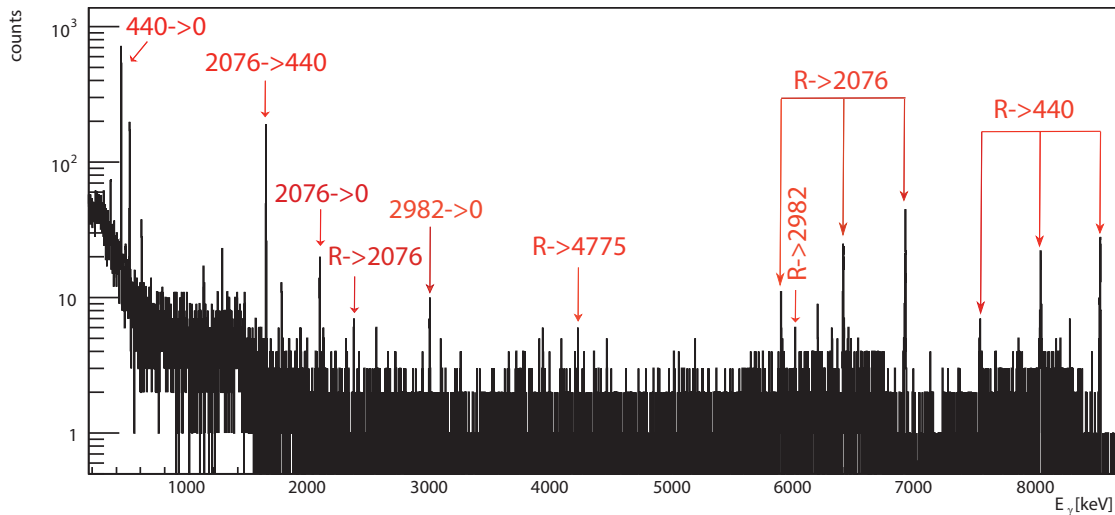


Figure 2. Observed γ -ray spectrum for the $E_p = 186$ keV resonance in $^{22}\text{Ne}(p,\gamma)^{23}\text{Na}$.

4 Results

For each resonance we studied the yield profile as a function of the proton beam energy. The latter has been changed in 1-2 keV steps.

The resonances at $E_R^{lab} = 159$, 186 and 256 keV have been detected for the first time. For the resonances at $E_R^{lab} = 71$, 104 and 215 keV an improved upper limit is being developed (table 1). In figure 2 the spectrum of the $E_R^{lab} = 186$ keV resonance is shown together with the identified ^{23}Na transitions.

5 Summary and outlook

The experimental setup for the $^{22}\text{Ne}(p,\gamma)^{23}\text{Na}$ resonances study has been developed and described. The density profile has been studied both with and without beam. The strength of the beam heating effect has been determined for neon gas using the resonance scan technique.

Three resonances have been detected for the first time in a direct experiment. The data analysis is still in progress, the final results will be presented in a forthcoming publication.

References

- [1] Marion et al., *Astrophys. J.*, **125**, 221 (1956)
- [2] R. Longland et al., *Phys. Rev. C* **81**, 055804 (2010)
- [3] J. Görres et al., *Nucl. Phys. A* **408**(2), 372 (1983)
- [4] J.R. Powers et al., *Phys. Rev. C* **4**, 2030 (1971)
- [5] S.E. Hale et al., *Phys. Rev. C* **65**, 015801 (2002)
- [6] C. Angulo et al., *Nucl. Phys. A* **656**, 3 (1999)
- [7] C. Iliadis et al., *Nucl. Phys. A* **841**, 251 (2010)
- [8] N. Mowlavi et al., *Astron. Astrophys.* **350**, 73 (1999)
- [9] S. Cristallo et al., *Mem. S.A.It.* **77**, 774 (2006)
- [10] C. Iliadis et al., *Astrophys. J. Suppl. Ser.* **142**, 105 (2002)
- [11] C. Broggini et al., *Annu. Rev. Nucl. Part. Sci.* **60**, 53 (2010)
- [12] C. Casella, et al., *Nucl. Phys. A* **203**, 706 (2002)
- [13] F. Cavanna, et al., *Eur. Phys. J. A* **50**, 179 (2014)
- [14] A. Formicola, et al., *Phys. Lett. B* **591**, 61 (2004)

